Journal of Translational Medicine

RESEARCH

Open Access

Protein modifications by advanced glycation end products (AGEs) in human clear cell renal cell carcinoma

Agnieszka Gęgotek[1*], Justyna Brańska-Januszewska[2], Paweł Samocik[3], Robert Kozłowski[3], Mariusz Koda[4], Neven Zarkovic[5], Elżbieta Skrzydlewska[1] and Halina Ostrowska[2]

Abstract

Background The development of cancer is often associated with altered glycolytic processes, resulting in the accumulation of highly reactive dicarbonyl compounds that promote protein modifications through advanced glycation end products (AGEs). This study aimed to quantify and identify the major AGE-modified proteins in clear cell renal cell carcinoma (ccRCC).

Methods A proteomic approach (SDS-PAGE/HPLC/MS–MS) with partial validation based on 2D-SDS-PAGE-Western blot was used to identify protein modifications by AGEs in cancer tissue samples of 16 patients with ccRCC compared to respective non-tumor kidney tissues of the same patients.

Results The findings revealed elevated levels of carboxymethylation/carboxyethylation along with the increased formation of pyrraline, argpyrimidine, and pentosidine on cysteine, lysine, or arginine residues in tumor tissues compared to matched non-tumor kidney tissue. Albumin was identified as a target for AGE modifications in its pre-proalbumin and mature forms. Most of the AGE-modified proteins in ccRCC tissues were involved in catalytic and binding functions, regulation, transcription and transport. These proteins were distributed throughout the cell, including the nucleus, as confirmed by immunofluorescence analysis. Of note, five of ten AGE-modified glycolytic enzymes were found exclusively in ccRCC tissues.

Conclusions This study demonstrates a distinct AGE-modified proteome in ccRCC compared to non-tumor tissue, with modifications frequently occurring within or near functional domainst. Therefore, further investigation into the mechanisms underlying AGE-protein adduct formation in renal carcinogenesis could help in understanding ccRCC development.

Keywords Advanced glycation end products (AGEs), Protein modification, Proteomics, Kidney disease, Tumor, Clear cell renal cell carcinoma (ccRCC)

*Correspondence:
Agnieszka Gęgotek
agnieszka.gegotek@umb.edu.pl
[1]Department of Analytical Chemistry, Medical University of Bialystok, Mickiewicza 2D, 15-222 Bialystok, Poland
[2]Department of Biology, Medical University of Bialystok, Mickiewicza 2A, 15-222 Bialystok, Poland
[3]Department of Oncological and General Urology, The Jędrzej Śniadecki Regional Polyclinical Hospital, Skłodowskiej-Curie 25, 15-278 Bialystok, Poland
[4]Department of General Pathomorphology, Medical University of Bialystok, Waszyngtona 13, 15-269 Bialystok, Poland
[5]Div. Molecular Medicine Laboratory for Oxidative Stress, Ruder Boskovic Institute, Zagreb, Croatia

Background

Clear cell renal cell carcinoma (ccRCC) is the most prevalent and most lethal subtype of kidney cancer diagnosed in adults, with its incidence steadily increasing in recent years [1]. Major risk factors contributing to ccRCC include obesity, diabetes, hypertension, and chronic kidney disease, as well as lifestyle, dietary, and environmental influences [2]. ccRCC originates from the epithelial cells of the proximal convoluted tubules, where inactivation or loss of the *von Hippel–Lindau* (VHL) tumor suppressor gene is commonly observed [2]. Loss of VHL function results in the stabilization of hypoxia-inducible factors (HIFs), leading to the upregulation of multiple genes involved in metabolic reprogramming, such as glucose transporters and glycolytic enzymes, as well as those promoting angiogenesis via vascular endothelial growth factor (VEGF), alongside with fatty acid and glycogen synthesis [3]. In addition, HIF signaling suppresses the tricarboxylic acid (TCA) cycle and oxidative phosphorylation (OXPHOS), contributing to a metabolic shift toward glycolysis [4]. Genomic and proteomic studies of ccRCC tissues have consistently shown the downregulation of mitochondrial enzymes associated with the TCA cycle and OXPHOS, together with overexpression of glycolytic enzymes such as aldolase A (ALDOA), lactate dehydrogenase A (LDHA), triosephosphate isomerase (TPI), glyceraldehyde-3-phosphate dehydrogenase (GAPDH), and pyruvate kinase M2 (PKM2), as well as enzymes of the pentose phosphate pathway (e.g., glucose-6-phosphate dehydrogenase, G6PD) and fatty acid biosynthesis [5]. Furthermore, glycolytic enzymes in ccRCC facilitate the conversion of glucose to lactate even in the presence of oxygen, a phenomenon known as the Warburg effect, which serves as the primary energy source for rapidly proliferating cancer cells [6, 7]. Due to these extensive metabolic alterations, ccRCC has been described as a "disease of cell metabolism" [8].

It is also well recognized that various types of post-translational modifications (PTMs) of glycolytic enzymes can redirect glycolytic intermediates into anabolic pathways, such as the pentose phosphate pathway (PPP), thereby supporting tumor cell proliferation [9, 10]. Among these, nonenzymatic protein glycation represents a stable and irreversible PTM that arises from the spontaneous reaction of glucose, fructose, or highly reactive dicarbonyl compounds, such as methylglyoxal (MGO), glyoxal (GO), and 3-deoxyglucosone (3-DG), with nucleophilic amino acid residues [11]. These dicarbonyls are primarily by-products of glycolysis but may also originate from lipid peroxidation, protein degradation, and dietary sources [12]. With reactivity up to 20,000 times greater than glucose, they rapidly modify lysine, arginine, and cysteine residues, resulting in the formation of advanced glycation end products (AGEs) [11, 12]. Major AGE-protein adducts include Nε-(carboxyethyl) lysine (CEL) and Nε-(carboxymethyl)lysine (CML), derived from MGO and GO, respectively, as well as S-(carboxyethyl)cysteine (CEC), S-(carboxymethyl)cysteine (CMC), pentosidine, and argpyrimidine [11], which may act as activators of the PPP pathway [13]. Consequently AGEs modify a wide range of extracellular and intracellular proteins, affecting their structure and function. Known targets include serum albumin, hemoglobin, type IV collagen and histones [14–16], as well as proteins involved in glycolysis, gluconeogenesis protein folding, transcription regulation, and antioxidant defense [17, 18]. MGO-induced modifications have been shown to impair the activity of key enzymes such as GAPDH, LDH, and SOD1 [19], alter chaperone function (e.g., Hsp27, Hsp90) [16], and influence chromatin architecture and gene transcription, particularly when glycation occurs in functional protein domains [20]. Moreover, AGE-protein adduct formation can also affect other PTMs of the protein by blocking the most reactive amino acid residues (including Cys and Lys), therefore changing the conformation of proteins, thus exposing other amino acids to further modifications [20, 21]. In addition to altering protein structure and function, AGEs can activate oncogenic signaling pathways (including NF-κB, HIF-1α, ERK, and AKT pathways) via interaction with their receptor (RAGE), thereby promoting cancer cell proliferation, migration, and invasion [22]. While AGE accumulation occurs gradually with aging, high levels are observed in various metabolic and age-related diseases, such as diabetes, obesity, cardiovascular diseases, and multiple tumor types [23], including breast, colon, liver, pancreatic, and thyroid carcinomas [24–26]. Despite the recognized presence of AGEs in tumors and their potential role in tumor biology, detailed information regarding the structure and functional impact of AGE-modified proteins is still limited.

Therefore, the present study aimed to quantify and identify the major AGE-modified proteins in human ccRCC tissue using a proteomics-based approach, with the goal of better understanding the role of protein glycation in renal cancer metabolism and progression.

Materials and methods

Patients and tissue samples

Cancerous and matched non-cancer kidney tissue samples were collected from 16 patients diagnosed with clear cell renal cell carcinoma (ccRCC) who underwent radical nephrectomy at the Department of Urooncology Surgery, Śniadecki Hospital in Białystok, Poland. Non-malignant kidney tissue samples were obtained from the distal edge of the surgical resection, at a minimum distance of 6 cm from the tumor margin. All patients signed the informed consent in accordance with the ethical approval granted

by the Human Care Committee of the Medical University of Białystok (approval no. R-I-002/43/2015). The mean age of the patients was 67.7 years (range: 52–84), and 66.7% were male. None of the patients had received chemotherapy or radiotherapy before surgery. Tumors were staged using the tumor-node-metastasis (TNM) classification system, and nuclear grade was assessed according to the Fuhrman grading criteria. The majority of samples were from tumors classified as pT1 ($n = 8$) and pT2 ($n = 3$), with five samples from pT3 stage tumors. Nine patients had no lymph node involvement (N0) or distant metastasis (M0); for the remaining seven patients, nodal and metastatic status was unknown at the time of surgery. All tumors, except one, were Fuhrman grade 2. Detailed clinicopathological characteristics of the ccRCC samples are provided in Additional File 1.

Both tumor and non-tumor tissue samples were preserved for subsequent analyses as snap-frozen in liquid nitrogen and stored at −80 °C until use, while the other specimens of the same tissue were formalin-fixed and paraffin-embedded for histological (hematoxylin–eosin staining) and immunohistochemical examination.

Immunofluorescence staining for AGEs

Formalin-fixed and paraffin-embedded slides (4 μm) were rehydrated using a series of decreasing ethanol concentrations, rinsed, and incubated with 5% normal donkey serum (Sigma-Aldrich Corp., St. Louis, MO, USA) at room temperature for 60 min to block the non-specific reactions. The sections were then washed three times with PBS and incubated with the primary rabbit anti-AGE polyclonal antibody (ab23722; Abcam, Cambridge, UK; 5 μg/mL) at 4 °C overnight, followed by incubation with donkey anti-rabbit IgG conjugated with Alexa Fluor488 (Molecular Probes, Eugene, OR, USA; 1:200 dilution) at room temperature in the dark for 60 min [27]. Nuclei were stained with 4',6-diamidino-2-phenylindole (DAPI, Sigma-Aldrich Corp., St. Louis, MO, USA). The negative control was performed by omitting the primary antibody to exclude non-specific binding of the secondary antibodies. After washing, the sections were covered with anti-fade fluorescent mounting medium (Medium Coverquick, Hygeco, OH, USA) and analyzed using a fluorescence microscope Nikon ECLIPSE Ti/C1 Plus (DAPI filter: Ex/Em 405/450 nm and FITC filter: Ex/Em 488/515 nm) and camera Nikon Digital Sight DS-Fi1. Images were imported into Image J software to obtain merged pictures. At least five randomly selected (not overlapping) microscopic fields per specimen were independently analyzed, with representative images presented for each group. The percentages of AGE-positive cells (nucleus and/or cytoplasm) were recorded.

Tissue homogenates preparation

The tissue samples (0.2 g) were washed several times with an ice-cold phosphate-buffered saline (PBS) and then mechanically homogenized with 200 μL cell lysis buffer (50 mmol/L Tris/HCl, pH 7.5, 1 mmol/L EGTA, 1 mmol/L EDTA, 1% Triton X-100, 0.25 mol/L sucrose) containing protease inhibitor cocktail (cOmplete Tablets, Mini EDTA-free Roche Diagnostics GmbH, Mannheim, Germany). Cellular debris was then removed by centrifugation at 15,000 g for 30 min at 4 °C. The total protein concentration of tissue homogenates was determined using the Protein Assay Dye Reagent Concentrate (Bio-Rad Laboratories Inc., Hercules, CA, USA) according to the manufacturer's protocol.

SDS–PAGE and Western blotting

Renal proteins (50 μg) from each extract were electrophoretically separated on a 10% SDS-PAGE gel. One gel was stained with Coomassie brilliant blue, and the other gel was used for immunoblotting. Proteins were transferred to a PVDF membrane and probed with the anti-AGE polyclonal antibody (ab23722; Abcam, Cambridge, UK; 1:500 dilution) [27] or β-actin (Sigma Chemical Co., St. Louis, MO) as an internal control. The immunoreactive proteins were visualized with an alkaline phosphate-conjugated anti-rabbit IgG as the secondary antibody (1:2000 dilution) and SIGMA FAST BCIP/NBT (bromochloroindolyl phosphate-nitro blue tetrazolium) substrate (Sigma-Aldrich, St. Louis, MO, USA). Images were captured with the Gel Doc™ XR + documentation system, and the intensities of the bands were analyzed by ImageLab software (Bio-Rad Laboratories Inc., Hercules, CA, USA).

Proteomic analysis of AGE-modified proteins

Kidney homogenates were denatured by mixing with Laemmli buffer supplemented with 5% 2-mercaptoethanol in a 1:1 ratio and heating at 95 °C for 10 min. Samples containing 30 μg of protein were separated on 10% SDS-PAGE gels and overnight stained with Coomassie Brilliant Blue R-250. Complete lanes were cut out of the gel, sliced into 8 sections (Additional File 2 showing the borders of the protein migration zones), washed, and following reduction with 10 mM DTT and alkylation with 50 mM iodoacetamide, in-gel digested overnight with trypsin (Promega, Madison, WI, USA). The obtained peptide mixture was extracted from the gel, dried, and dissolved in 5% ACN (with 0.1% formic acid). To separate peptides, Ultimate 3000 (Dionex, Idstein, Germany) with a 150 mm × 75 μm PepMap RSLC capillary analytical C18 column (Dionex, LC Packings) was used. Peptides were analyzed using a QExactive HF mass spectrometer with an electrospray ionization source (ESI) (Thermo Fisher Scientific, Bremen, Germany). The mass spectrometer

was externally calibrated and operated in positive mode and data-dependent mode. Survey MS scans were conducted in the 200–2000 m/z range with a resolution of 120,000. In subsequent scans, the top ten most intense ions were isolated, fragmented, and analyzed at 30,000 resolution. The detailed method parameters were described in Additional File 3.

Raw data generated from LC–MS/MS analysis were processed using Proteome Discoverer 2.0 (Thermo Fisher Scientific, Bremen, Germany), and input data were searched against the UniProtKB—SwissProt database (taxonomy: *Homo sapiens*, release 2018-04). The detailed parameters of the protein identification were described in Additional File 3. Only proteins with at least two unique peptides identified were taken for further analysis. Cysteine and lysine carboxymethylation/carboxyethylation (CMC/CEC and CML/CEL), pyrraline, argpyrimidine, and pentosidine formation on lysine or arginine were set as a dynamic modification [28]. The modified protein quantification was done based on the peak intensity analysis. Because trypsin used for digestion specifically cuts proteins only after unmodified amino acids, all identified modifications (especially on cysteine residues) were determined only qualitatively and semi-quantitatively.

Statistical analysis

Results comparing means of single parameters (including the percentage of positively stained cells and level of AGE-modified proteins) were analyzed for statistical significance with Student's t-test (following testing normality of the distribution of the results with the Shapiro–Wilk test) using the GraphPad Prism® program (GraphPad Software). The value of $p < 0.05$ was considered significant. Proteomic results from individual protein label-free quantification were subjected to data imputation (missing values were replaced by 1/10 of the minimal positive values of their corresponding variables), normalized by the sum of the protein intensities, and log-transformed using open-source software MetaboAnalyst 5.0 (http://www.metaboanalyst.ca) [29]. The same softwa re was used for biostatistical analysis (the false discovery rate (FDR) < 5%). Biological and molecular functions of proteins were identified using the Panther Classification System (http://pantherdb.org) [30]. Observed differenc es in protein expression were validated according to the Clinical Proteomic Tumor Analysis Consortium-Clear Cell Renal Cell Carcinoma (CPTAC-CCRCC) collection [31].

Results

Localization of total AGE-modified proteins in renal tissues from ccRCC patients

The patterns of renal proteins, separated by SDS-PAGE and visualized via Coomassie Brilliant Blue staining or immunoblotting with anti-AGE antibodies, are presented in Fig. 1 and in Additional File 2. Coomassie-stained gels revealed multiple protein bands both in ccRCC tumors and matched non-tumor renal tissue samples for all patients, with most proteins exhibiting molecular weights between 80 and 19 kDa. A prominent band, corresponding to albumin (~ 68 kDa), was consistently detected in both tumor and non-tumor tissues. Notably, three bands—ranging from ~ 32 to 35 kDa and ~ 19 kDa—were more intense in tumor tissues compared to adjacent non-tumor counterpart tissues (Fig. 1A). At the same time, Western blot analysis using anti-AGE antibodies revealed strong immunoreactivity with the 68 kDa band and a weaker reactivity with several additional proteins, including a visible band at ~ 25 kDa. Minor AGE immunoreactivity was also observed in high-molecular-weight proteins (> 100 kDa) (Fig. 1B).

Immunohistochemical analysis further illustrated the distribution of AGE-modified proteins in both ccRCC and non-tumor renal tissue specimens (Fig. 1C). In ccRCC tissues, diffuse AGE staining was predominantly cytoplasmic in cancer cells but was also detected in tumor-associated vasculature. Additionally, nuclear AGE staining was observed in a subset of tumor cells. Non-tumor kidney tissues also displayed diffuse AGE immunoreactivity in the cytoplasm of cortical tubular epithelial cells, while glomerular cells were largely negative, except for arterioles. Occasional nuclear staining was present in tubular epithelial cells. Notably, strong perinuclear staining was observed in some tubular epithelial cells but was absent in tumor cells. Quantitatively, positive AGE staining was detected in approximately 60% of proximal tubular epithelial cells and 25–30% of ccRCC cells, representing statistically significant ($p < 0.05$) differences between these groups (Fig. 1D). The specificity of immunostaining was confirmed by the absence of immunoreactivity in control sections incubated without primary antibodies (Additional File 4). In summary, diffuse AGE immunohistochemical staining was observed in the cytoplasm and nucleus of tumor cells and nonmalignant tubular epithelial cells, indicating that AGE-modified proteins are also formed intracellularly.

Semi-quantitative analysis of AGE-protein adducts in ccRCC and non-tumor renal tissues

The levels of AGE-modified proteins differed markedly between ccRCC tissues and matched non-tumor renal samples (Fig. 2). Because albumin was the most intensely modified protein, its quantification is presented separately (Fig. 2A). Although inter-individual variability was observed, AGE-modified albumin levels were significantly higher in non-tumor tissues compared to their corresponding ccRCC samples ($p < 0.05$). The majority, i.e., 13 out of 16 cases, exhibited at least a 1.5-fold higher

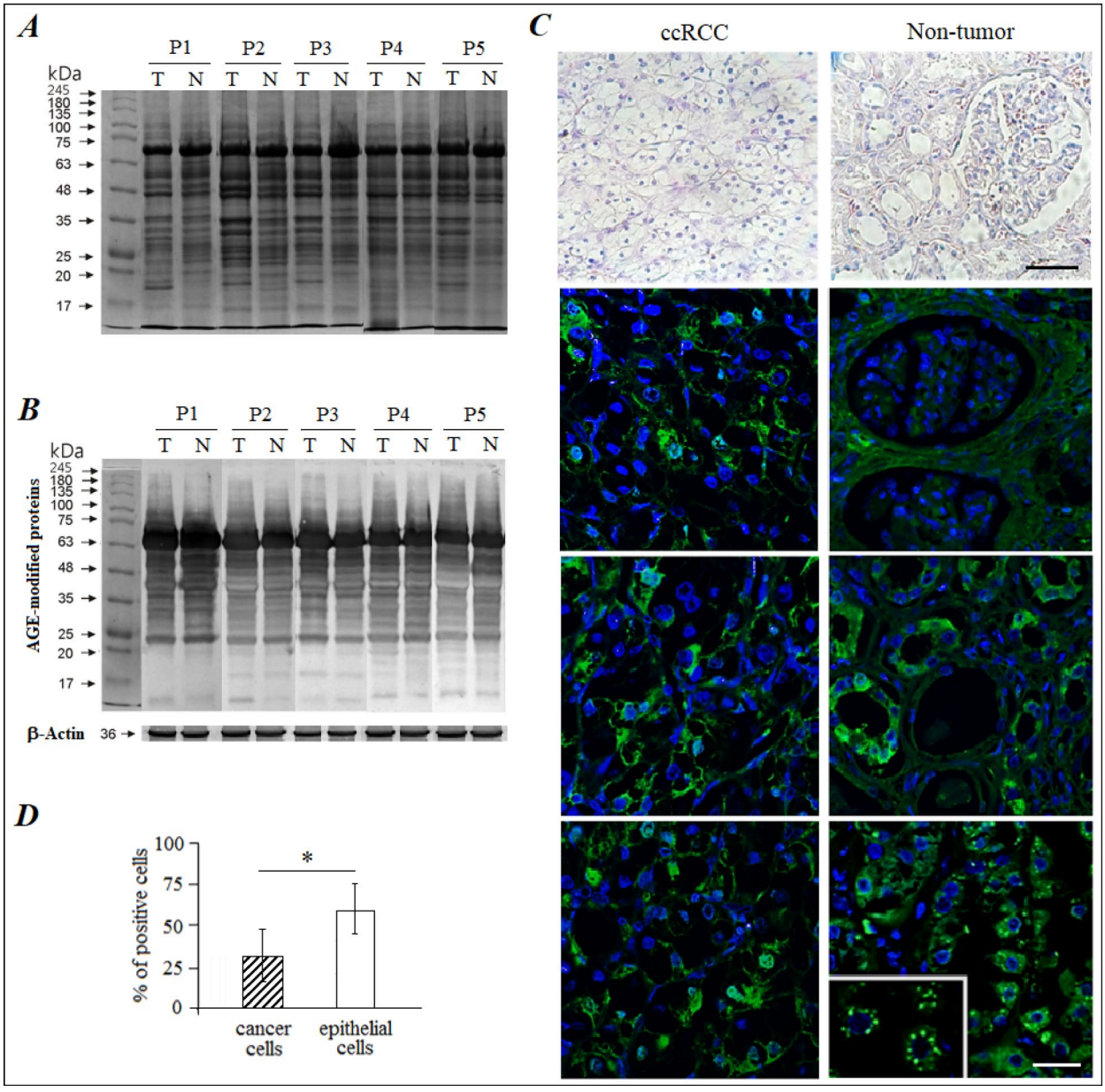

Fig. 1 **A**, **B** SDS-PAGE analysis and Western blotting of anti-AGE immunoreactive proteins in clear cell renal carcinoma (ccRCC) (tumors, T) and corresponding non-tumor (N) renal tissues from 16 patients. Representative patterns of proteins after staining with Coomassie Brilliant Blue R-250 **(A)** and after immunoblotting with the polyclonal anti-AGE antibody are shown **(B)**. Results obtained for the first 5 patients in different stages of the disease are presented (P1-P2, pT1N0M0; P3-P4, pT2N0M0; P5, pT3NxMx). The size of the molecular weight markers is indicated in kilodaltons on the left of the panels. The remaining results are included in Additional File 2. **C** Immunofluorescence analysis of the localization of AGEs (green) in ccRCC (left panels) and non-tumor renal tissues (right panels) of the three patients, respectively. Nuclear counterstaining (blue). Representative images are shown at the original magnification (600×). Upper panels show histology of renal tumor nest (left panel) and renal cortex (right panel) on hematoxylin and eosin stain (H&E). Scale bar: 50 µm. **D** The percentage of AGE-positive renal tumor cells and non-malignant epithelial cells per 20 different slides, was detected by immunofluorescence staining. Mean values ± SD are presented with statistically significant differences (*) comparing tumor cells and non-malignant epithelial cells ($p < 0.05$).

AGE-albumin level in normal than in cancer tissue specimens, whereas only three samples (patients 1, 7, and 11) showed equal levels in tumor and non-tumor tissues.

In contrast, total levels of other AGE-modified proteins were generally higher in ccRCC tissues ($p < 0.05$) (Fig. 2B). The expression of each protein was normalized to analyze the level of modification without the influence of differences in protein expression between matched tumor and non-tumor samples. Thus, 10 of the 16 tumor samples (62.5%) exhibited more than a 1.5-fold increase in total AGE-modified protein levels above their matched non-tumor tissues. In the remaining six patients, four

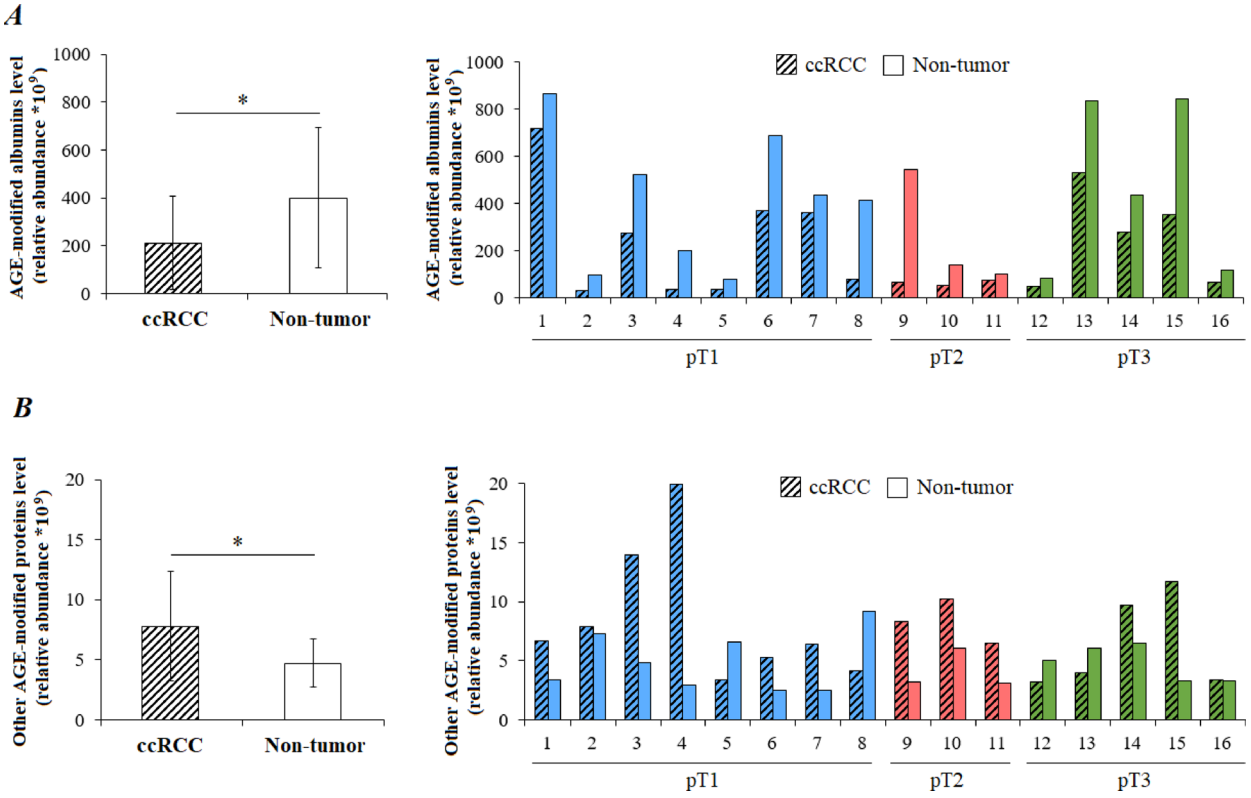

Fig. 2 Semiquantitative analysis of AGE-modified albumins **(A)** and other AGE-modified protein levels **(B)** in clear cell renal carcinoma (ccRCC) and non-tumor renal tissue samples of 16 patients (comparison of peak intensities between ccRCC and non-tumor tissue). The left panel shows the mean ± SEM values in ccRCC tissues relative to non-tumor renal tissues (*$p < 0.05$; $n = 16$). Right panel shows results obtained for individual ccRCC patients grouped according to the TNM stage: P1-P3, pT1aN0MO; P4-P6, pT1bN0M0; P7-P8, pT1bNxMx; P9-P10, pT2aN0M0; P11, pT2aNxMx; P12-P13, pT3aN0M0; P14-P16, pT3cNxMx

(patients 5, 8, 12, and 13) had lower AGE-protein adduct level in tumor tissues, and two (patients 2 and 16) showed similar levels between tumor and non-tumor tissues. Furthermore, in the majority of ccRCC samples (13 out of 16; 81%), proteins modified by at least two different AGE adduct types were detected at 1.5- to tenfold higher levels if compared to their non-tumor counterparts (Table 1). Only one patient (no. 12) exhibited markedly lower or comparable levels of all detected AGE adducts in ccRCC tissue than in non-tumor renal tissue. Levels of individual AGE-protein adducts in ccRCC and matched non-tumor renal tissues of each patient are presented in Additional File 5. No clear associations were observed between AGE-protein adduct levels and clinical parameters such as TNM stage, patient age, or sex. Additionally, levels of AGE-modified proteins (both albumin and other modified proteins) did not correlate with pT stage of the patients ($p > 0.05$ for both) (Additional File 6). Overall, ccRCC samples exhibited lower levels of AGE-albumin adducts but higher levels of AGE adducts on other proteins.

Albumin modifications by AGEs in ccRCC patients

Mass spectrometry (MS) analysis of a prominent protein band (~70 kDa) separated by SDS-PAGE confirmed that identified serum albumin (UniProt P02768) as the main AGE-modified protein in clear cell renal cell carcinoma (ccRCC) tissues as well as in matched non-tumor renal tissue samples. Both pre-proalbumin (calculated molecular mass: 69.4 kDa) and mature serum albumin (calculated molecular mass: 66.5 kDa) were found to contain AGE adducts.

AGE modifications found on pre-proalbumin predominantly consisted of cysteine-derived adducts (CEC and/or CMC), followed by arginine-derived compounds (pentosidine and/or argpyrimidine) (Fig. 3A). The localization of these AGE adducts within the pre-proalbumin structure is illustrated in Fig. 3B. Modifications were detected at four arginine residues (R-19, R-246, R-469, R-545), with R-19 located in the pro-peptide sequence, and at seven cysteine residues (C-86, C-99, C-201, C-224, C-277, C-500, C-511) capable of forming disulfide bonds. Among these eleven AGE-modified sites, three (R-19, R-496, and C-500), indicated by asterisks, were exclusively observed on pre-proalbumin from ccRCC samples, whereas the remaining eight sites were present

Table 1 Changes in the levels of proteins modified by individual AGEs in clear cell renal carcinoma (ccRCC) tissues over the matched non-tumor renal tissues of 16 patients

No	TNM stage	Levels of proteins modified by individual AGEs in tumor tissue (fold change)*						
		CEL	CML	CEC	CMC	Pyrraline	Arg-p	Pento-s
1	pT1aN0M0	↑↑	↑	↑	↑	↑	↓	↔
2	pT1aN0M0	↓	↓	↔	↑↑	↔	↑	↑
3	pT1aN0M0	↑	↑	↔	↑	↑↑↑	↑	↑
4	pT1bN0M0	↑↑↑	↑↑↑	↑	↑	↑	↑	↑↑
5	pT1bN0M0	↓↓	↓↓	↓	↔	↑	↑	↓
6	pT1bN0M0	↓	↑	↑	↑↑↑	↔	↓	↑↑
7	pT1bNxMx	↑	↑	↑	↑↑	↑	↑	↔
8	pT1bNxMx	↓↓	↓↓↓	↔	↑	↔	↓↓	↔
9	pT2aN0M0	↑↑	↑	↑	↑	↑	↑↑	↔
10	pT2aN0M0	↔	↑	↑	↑↑	↔	↑↑	↑
11	pT2aNxMx	↑	↔	↑	↑	↑	↓	↔
12	pT3aN0M0	↓↓	↔	↓	↔	↔	↓↓	↔
13	pT3NxM0	↔	↓	↔	↔	↓	↑↑	↓
14	pT3NxMx	↑	↑	↑	↑↑	↑	↑	↓↓
15	pT3cNxMx	↓	↑	↑	↑	↓↓	↓↓	↑↑↑
16	pT3cNxMx	↓	↓	↔	↑	↑	↑	↑

*AGE-modified proteins (peptides) were quantified by LC/MS/MS-based methodology. All changes are expressed as fold-change relative to a non-tumor renal sample, as follows: (↑) or (↓): 1.5-4-fold; (↑↑) or (↓↓): 4.1-10-fold; (↑↑↑) or (↓↓↓): 10.1-20-fold increase or decrease, respectively; (↔): unchanged; shaded table cells: increase. Abbreviations: Arg-p, argpyrimidine; CEL-carboxyethyl-lysine; CML, carboxymethyl-lysine, CEC, carboxyethyl-cysteine; CMC, carboxymethyl-cysteine; Pento-s, pentosidine; Pyr, pyrraline.

on pre-proalbumin derived from both ccRCC and non-tumor renal samples.

In contrast, AGE modifications on mature serum albumin were exclusively lysine-derived compounds, including CEL and/or CML, as well as pentosidine and/or pyrraline (Fig. 4A). A total of 12 AGE-modified lysine residues were identified on albumin from both ccRCC and non-tumor renal tissues (Fig. 4B). Notably, four of these modified lysines (K-199, K-233, K-276, and K-281) were located at the drug-binding site Sudlow I within subdomain IIA (residues 150–292), while modification at K-439 was detected at Sudlow site II in subdomain IIIA (residues 384–489). Additionally, lysine 525, the primary site of albumin glycation in vivo, was modified by CML, CEL, or pentosidine in both ccRCC and non-tumor renal tissues. The general tendency to form AGE adducts on albumin was based on Lys modification in both ccRCC and non-tumor samples, whereas AGE modifications of pre-proalbumin mainly concerned Cys and Arg and differentiated ccRCC and non-tumor samples by the positions of the modified residues of these amino acids.

Qualitative MS identification of other AGE-modified proteins

Proteomic analysis, excluding AGE-albumin adducts, identified 113 AGE-modified proteins in ccRCC samples and 99 AGE-modified proteins in matched non-tumor renal samples from at least ten patients (Fig. 5A). In total, 70 AGE-modified proteins were common to both ccRCC and non-tumor renal tissues, while 43 and 29 proteins were found unique either in tumor or in non-tumor samples, respectively. A comprehensive list of all 142 AGE-modified proteins, including their UniProt accession numbers, molecular weights, peptide sequences, and AGE modification sites, is provided in Additional File 7. The majority of identified proteins had molecular weights (MW) ranging from 20 to 150 kDa (Fig. 5B). The patterns of AGE modifications were similar between ccRCC and non-tumor renal tissues, predominantly involving lysine-derived adducts (CML, CEL, pentosidine, and/or pyrraline) and cysteine-derived adducts (CEC and CMC), followed by arginine-derived adducts (argpyrimidine and pentosidine) (Fig. 5C). The majority of proteins ($n = 93$) contained a single predicted AGE-modified site, while 49

A

Cys-derived adducts	Modified sites	Tumor	Non-tumor
CEC	C-99, C-201, C-277	Yes	Yes
	C-500, C-511	Yes	No
CMC	C-86, C-224, C-511	Yes	Yes
	C-201	Yes	No

Arg-derived adducts	Modified sites	Tumor	Non-tumor
Pentosidine	R-19, R-246	Yes	No
Argpyrimidine	R-246, R-545	Yes	Yes
	R-469	Yes	No

B

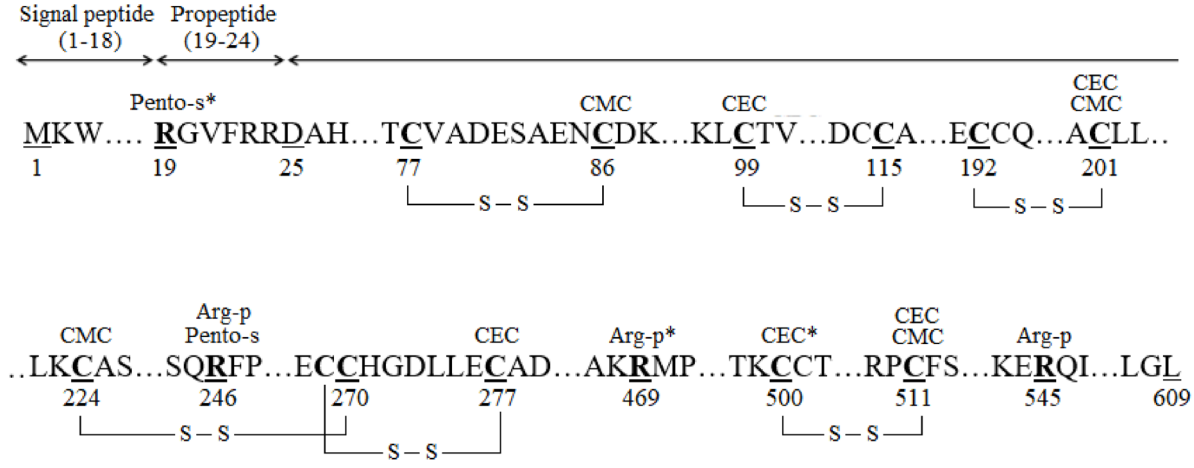

Fig. 3 **A** AGE adducts in pre-proalbumin from clear cell renal carcinoma (ccRCC) and non-tumor renal tissues found in samples from at least 12 out of 16 studied patients. **B** The sequence of pre-proalbumin (609 amino acids) from the UniProt database with regions of the signal peptide, propeptide, and mature albumin. The identified AGE-modified arginines (R) and cysteines (C) are bolded and their positions in the sequence are underlined. Asterix indicates AGE adducts found on pre-proalbumin from the ccRCC samples only. Abbreviations: CMC, carboxymethyl-cysteine; CEC, carboxyethyl-cysteine Pento-s – pentosidine; Arg-p, argpyrimidine

proteins carried two or three modified sites (Additional File 7).

Analysis of the subcellular localization and functions of the AGE-modified proteins revealed that most of them were intracellular components, with only a minority being extracellular (Fig. 6A). Subcellular distribution primarily involved cytoplasmic compartments (cytosol, mitochondria, cytoskeleton, etc.), followed by the nucleus and plasma membrane. Notably, the abundance of nuclear proteins was higher in ccRCC tissues compared to non-tumor renal tissues, in accordance with immunofluorescence findings (Fig. 1C).

Molecular function annotation indicated that the majority of AGE-modified proteins identified in ccRCC, and non-tumor renal samples possessed catalytic and binding activities, followed by molecular function regulators, transporters, transcription regulators, and structural proteins (Fig. 6B). AGE-modified proteins with transcription regulator activity were more prevalent in ccRCC samples (6.0%) than in non-tumor samples (1.4%). Other functional groups showed comparable representation between the two sample types.

AGE-modified proteins were further categorized according to their biological activities (Table 2). The largest group comprised proteins involved in transcription regulation and RNA processing ($n = 20$), half of which were modified exclusively in ccRCC tissue. Another group of modified proteins was involved in signaling

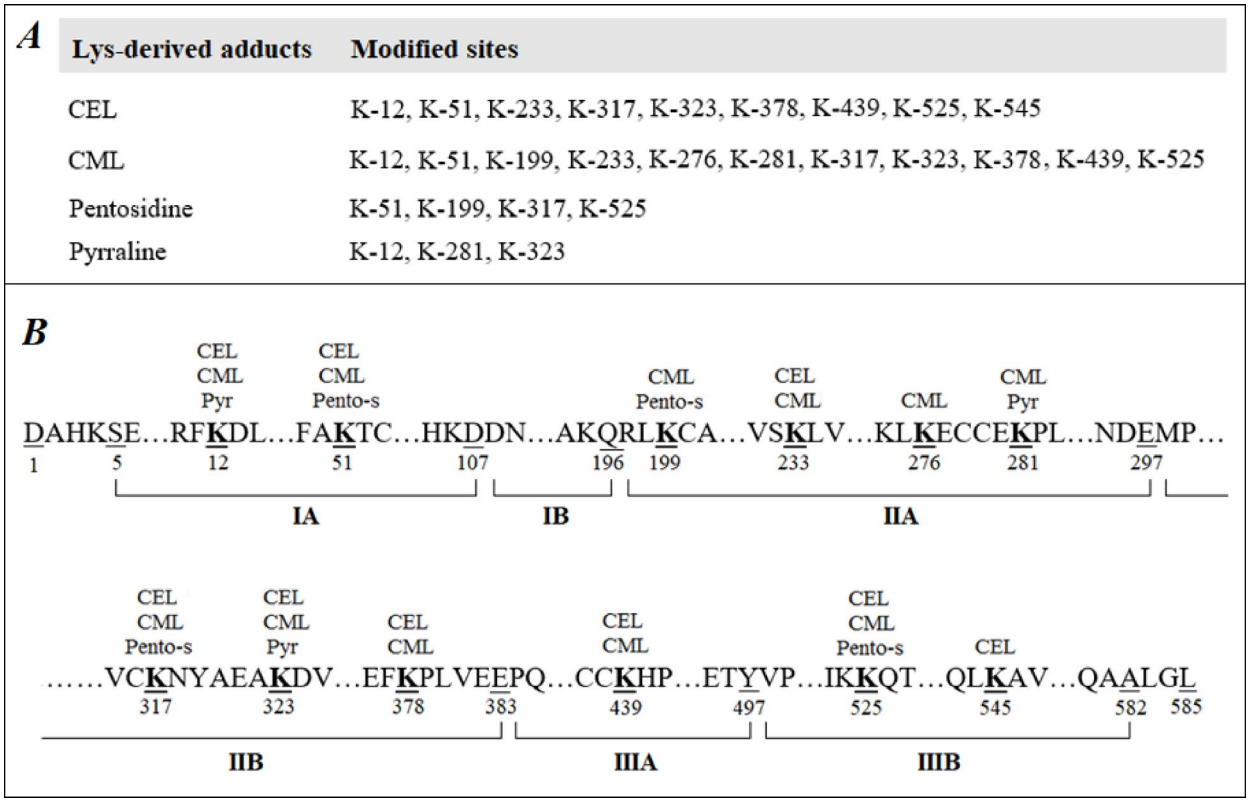

Fig. 4 **A** Lysine-derived AGE adducts found on mature serum albumin from clear cell renal carcinoma (ccRCC) and non-tumor renal tissues found in samples from at least 12 out of 16 studied patients. **B** The sequence of serum albumin (585 amino acids; 66.5 kDa) from the UniProt database and the sites of AGE modifications. AGE-modified lysine (K) residues are bolded and their positions in albumin subdomains are underlined. Abbreviations: CEL, carboxyethyl-lysine; CML, carboxymethyl-lysine; Pento-s, pentosidine; Pyr, pyrraline

pathways ($n = 10$; 6 of them modified exclusively in ccRCC tissue), glycolysis ($n = 10$; 5 of them modified exclusively in ccRCC tissue), oxidation–reduction processes ($n = 10$; 4 of them modified exclusively in ccRCC tissue), and protein folding ($n = 9$; 3 of them modified exclusively in ccRCC tissue). Additional categories included proteins related to ubiquitination and degradation ($n = 5$; 2 of them only in ccRCC tissue), cytoskeleton organization ($n = 4$; 1 of them only in ccRCC tissue), DNA replication and repair ($n = 3$; 2 of them only in ccRCC tissue), fatty acid metabolism ($n = 3$; 1 of them only in ccRCC tissue), immune responses ($n = 3$; 2 of them only in ccRCC tissue), protein biosynthesis ($n = 3$), mitochondrial ATP synthesis ($n = 3$), ion transport ($n = 3$), the tricarboxylic acid (TCA) cycle ($n = 2$), and blood coagulation ($n = 2$). The analysis of functional domains in these proteins showed that 41 of them had AGE adducts at sites or close to the functional domains essential for substrate binding, catalytic activity, interactions with other proteins or nucleic acids, disulfide bond formation, and/or post-translational modifications (i.e. acetylation, ubiquitination, or sumoylation) (Additional File 8). The list of the 21 AGE-modified proteins unique to ccRCC tissues, including the positions of modified sites, and functional domains is provided in Table 3.

Discussion

Cancer cells, including ccRCC, are characterized by uncontrolled proliferation and elevated energy demands. This energy is primarily supplied through aerobic glycolysis, which leads to increased glucose uptake and generation of glycolytic byproducts, such as methylglyoxal (MGO) and glyoxal (GO). These reactive dicarbonyl compounds can react with proteins, resulting in the formation of irreversible AGEs. The AGE-protein adducts have been previously detected not only in tumors [12] but also in aging kidney and renal diseases such as diabetic nephropathy and chronic kidney disease (CKD), both of which are recognized risk factors for renal tumor development [32], while CKD is frequently associated with locally advanced renal carcinoma [33].

In this study, we present the first comparative analysis of AGE-modified proteins in tumor tissues from ccRCC patients and matched non-tumor renal tissues. Immunohistochemical analysis revealed the widespread AGEs presence both in the cytoplasm and nucleus of carcinoma

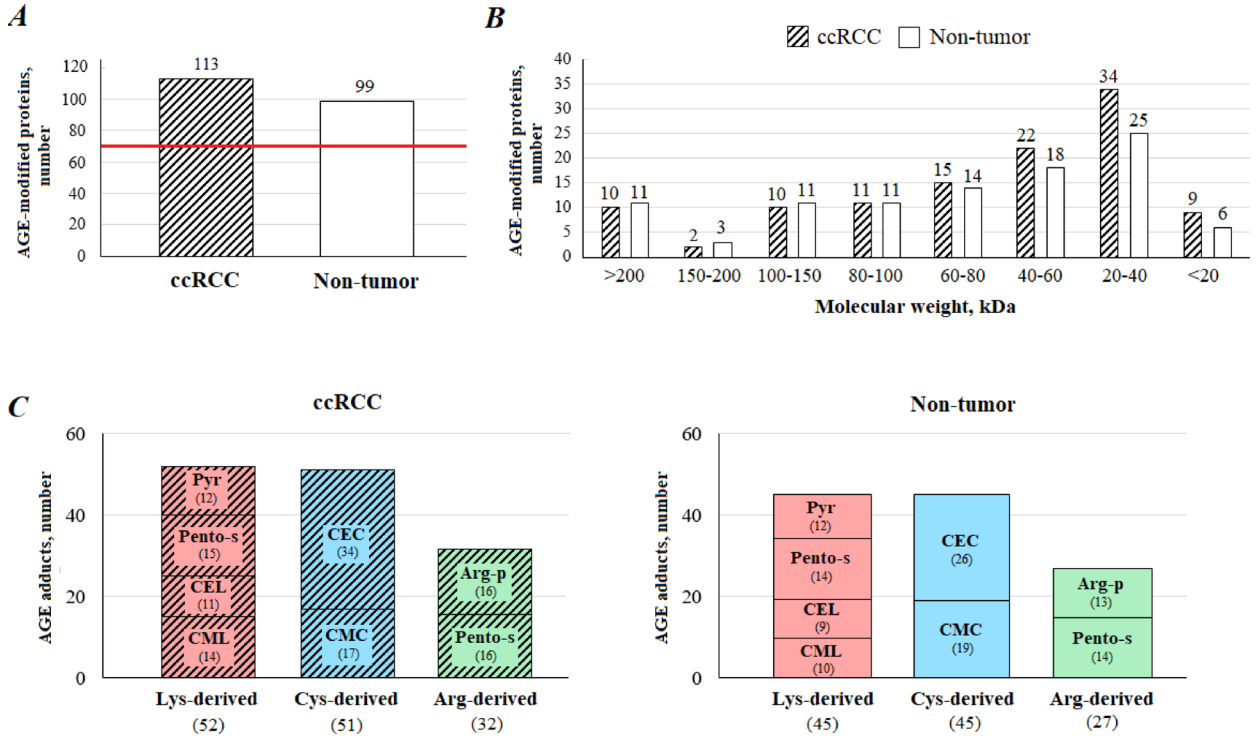

Fig. 5 **A** A total number of AGE-modified proteins identified in clear cell renal carcinoma (ccRCC) and non-tumor renal tissue samples found in samples from at least 12 out of 16 studied patients. The red line indicates the number of AGE-modified proteins common in both ccRCC and non-tumor renal tissues ($n = 70$). **B** Distribution of the protein molecular weights based on the UniProt database; the number over each box indicates the total number of AGE-modified proteins. **C** The number of lysine, cysteine, and arginine -derived AGE adducts in the 113 proteins identified in ccRCC samples (left panel) and the 99 proteins identified in the non-tumor renal samples (right panel). In parenthesis, the number of individual AGE adducts is reported. Abbreviations: CML, carboxymethyl-lysine; CEL, carboxyethyl-lysine; Pento-s, pentosidine; Pyr, pyrraline; CMC, carboxymethyl-cysteine; CEC, carboxyethyl-cysteine; Arg-p, argpyrimidine

cells and non-malignant kidney cells, suggesting that AGE-modified proteins are formed intracellularly.

Our proteomic approach further identified the potential protein targets of AGE modifications in ccRCC and non-tumor renal tissues. Some of these proteins have previously been reported as susceptible to non-enzymatic glycation in vivo and in cancer cell lines exposed to methylglyoxal or glyoxal [17, 23]. Therefore, we discuss the potential functional consequences of AGE modifications on identified proteins particularly about their possible roles in tumor development.

Albumin and pre-proalbumin modifications by AGEs

Serum albumin (P02769) was the most abundant AGE-modified protein in both ccRCC and non-tumor renal tissues. It might be related to the fact that albumin is taken up from the circulation and metabolized in renal proximal tubule cells [34]. Moreover, albumin accumulates in the tumor interstitium due to increased capillary permeability and the lack of lymphatic drainage and is then internalized and degraded by cancer cells as a source of amino acids and energy [35]. Furthermore, AGE-modified albumin, if not degraded, tends to aggregate and accumulate within cytoplasmic inclusion bodies, potentially triggering cell death [36]. Indeed, we observed a strong punctate AGE staining in many non-malignant renal epithelial cells, but not in ccRCC cells (Fig. 1), which may reflect accumulation of AGE-modified albumin in non-tumor renal tissues, explaining higher relative levels of AGE-modified albumin there. On the other hand, perhaps the AGE-modified albumin released from damaged kidney cells or necrotic cancer cells may be utilized to promote proliferation of ccRCC cells through binding to the receptor for AGEs (RAGE) that is overexpressed in renal carcinoma cells [37]. This option should be further studied to explain differences in the formation and biological activities of AGEs, in particular albumin adducts, between normal kidney epithelium and the malignant counterpart cells.

Mature serum albumin contains several lysine and arginine residues that are known target sites for glycation and MGO modifications both in vitro and in vivo [14, 38]. Our analysis revealed AGE modifications on twelve lysine residues of serum albumin from both tissue types, with six of these located in known drug-binding sites (Fig. 4), which potentially may affect albumin's biological functions.

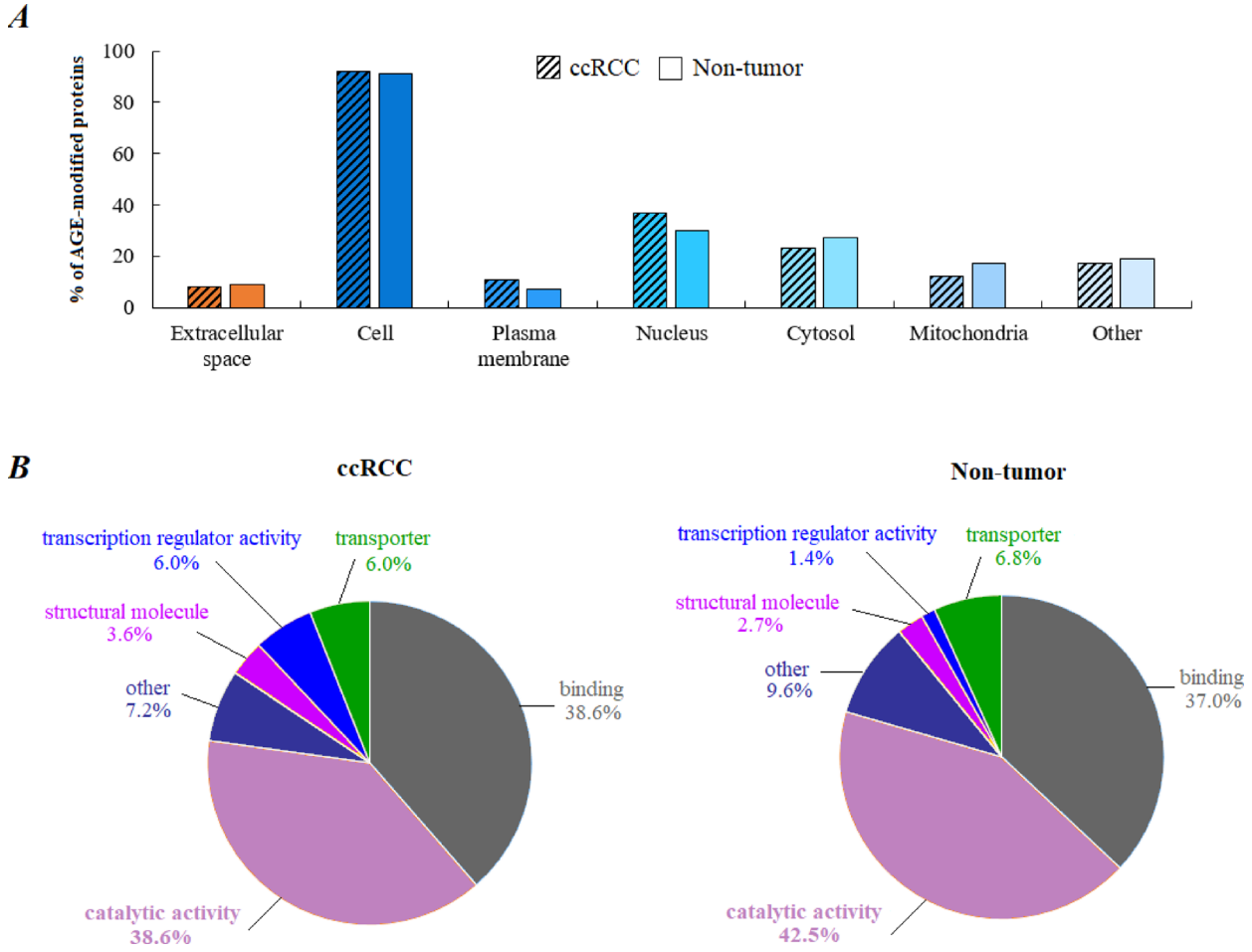

Fig. 6 Classification of proteins that formed AGE adducts in clear cell renal carcinoma (ccRCC) and non-tumor renal tissue samples based on **(A)** distribution and **(B)** molecular function according to the UniProt database. PIE charts show the results of GO (Gene Ontology) analysis within the Panther Classification System

Interestingly, AGE-modified pre-proalbumin was also identified in both tissue types. Although predominantly synthesized in hepatocytes, albumin gene expression has been detected at low levels also in the kidney and is up-regulated following acute injury [39, 40]. Therefore, local synthesis and subsequent post-translational glycation may explain the presence of AGE-modified pre-proalbumin in non-tumor renal tissues of our patients, while possible synthesis, not only accumulation, of albumin by ccRCC cells is an attractive option for further studies on the relevance of albumin and its AGE-modifications for development of ccRCC. That could be highly relevant because AGE-adducts were more abundant in pre-proalbumin from ccRCC tissues compared to non-tumor renal tissues. These included cysteine-derived CEC and/or CMC, as well as arginine-derived argpyrimidine and pentosidine. According to the Uniprot database, six of the seven cysteine residues that were modified by AGEs (Fig. 3) participate in the formation of intramolecular disulfide bonds in native albumin. These disulfide bonds are rapidly formed in the endoplasmic reticulum and are essential for the structural stability of mature albumin in circulation [41]. Consequently, AGE modification of cysteines in pre-proalbumin may interfere with proper disulfide bond formation, potentially impairing albumin maturation and function. Furthermore, AGE modification of pre-proalbumin in ccRCC was detected exclusively at Arg-19, located within the pro-peptide sequence ^{19}Arg-Gly-Val-Phe-Arg-Arg^{24}. Previous studies have shown that the substitution of either Arg-23 or Arg-24 disrupts the final intracellular processing of albumin [42]. However, the functional consequence of Arg-19 modification by pentosidine within the pro-peptide region remains to be elucidated.

Intracellular proteins modified by AGEs in ccRCC patients

The majority of AGE-modified proteins identified in the tumor and non-tumor renal samples are located in the cytoplasm and nucleus (Fig. 6). Most of them possess catalytic or binding activity and are involved in key

Table 2 AGE-modified proteins were identified in clear cell renal carcinoma (ccRCC) tissues and non-tumor renal tissue samples of 16 patients grouped according to their main functions in biological processes

Proteins related to:	AGE modification		Proteins related to:	AGE modification	
	T	N		T	N
Glycolysis			**Protein biosynthesis**		
ALDOA, LDH-A, PGK1	Yes	Yes	ELP6, EIF3CL	Yes	Yes
PFKP, TPI1, GAPDH, ENO1, PKM2	Yes	No	EEF1A1	No	Yes
ENO2, GALM	No	Yes	**Protein folding**		
Mitochondrial ATP-synthesis	HSPD1, PPIAL4H, PHB,	Yes	Yes		
ATP8, ATP5F1A, UCP2	Yes	Yes	HSP90AB1, PDIA3, PSMD5	Yes	No
Citrate cycle (TCA cycle)	DNAJC10, HEL-S-72p	No	Yes		
ACO2, SUCLG2	No	Yes	**Protein ubiquitination and degradation**		
Lipid metabolic processes	RMND5A, GLMN	Yes	Yes		
ACSL1, PITPNM2	Yes	Yes	UBA5, PSMD5	Yes	No
ACAT1	No	Yes	UBR3	No	Yes
Oxidation–reduction processes	**Signaling pathway**				
CAT, GPX1, HEL-S-2a	Yes	Yes	RHPN1, ITK, TNL1, YWHAZ	Yes	Yes
CYP2C9, GPX4, GRHPR, HEL-S-44	Yes	No	CHRM2, ANKLE2, FLNA, MAP3K6,	Yes	No
AOX-1	No	Yes	KLHDC8A, CRIPTO	Yes	No
DNA replication and repair			**Cytoskeleton organization**		
REV1	Yes	Yes	MYH2, MYBPH, TNL1	Yes	Yes
SMG1, GAPDH	Yes	No	FNLA	Yes	No
Transcription regulation and RNA processing	**Ion transport**				
ABT1, CREM, CHD6, HNRNPA3,	Yes	Yes	CLIC4, HEL-S-71p	Yes	Yes
BARX1, HNRPA1, AGO2, RBM26,	Yes	Yes	HPX	No	Yes
DDX39B, UTY	Yes	Yes	**Immune responses**		
			C9	Yes	Yes
DDX19B, ESRP2, MED17, REXO4,	Yes	No	CF1, CPN2	Yes	No
SRSF4, SHOX2, STAT2, ENO1,	Yes	No	**Blood coagulation**		
GAPDH, PKM2	Yes	No	A2M, APOH	Yes	Yes

Used protein symbols come from the UniProtKB (2023), the full protein names and accession numbers are shown in Additional File 8. Proteins that formed AGE adducts exclusively in ccRCC tissue are marked in red. Abbreviations: T, tumor samples; N, non-tumor renal samples

biological processes, including glycolysis, transcriptional regulation, redox homeostasis, protein folding, protein ubiquitination, signal transduction, cytoskeleton organization, and intracellular transport. Of note, in many of these proteins AGE adducts were detected within, or in close proximity, to key functional domains (Table 3), suggesting that this non-enzymatic modification may influence their structure and function.

Glycolytic enzymes

In the present study, ten glycolytic enzymes were found to contain AGE adducts (Table 2), consistent with previous studies indicating that glycolytic enzymes are primary targets of non-enzymatic glycation in cancer cell lines exposed to reactive dicarbonyls, as well as in the diabetic rat kidney [43, 44]. Notably, five AGE-modified glycolytic enzymes uniquely detected in ccRCC samples included the platelet isoform of phospho-fructokinase (PFKP), triosephosphate isomerase (TPI1), glyceraldehyde 3-phosphate dehydrogenase (GAPDH), α-enolase 1 (ENO-1), and pyruvate kinase (PKM2), with modifications localized within functional domains (Tables 2 and 3). As shown in Fig. 7, while ENO-1 and PKM2 are the most important enzymes participating in the glycolytic acquisition of pyruvate in cells, we found that ENO-1 was modified by CML and/or pentosidine on Lys-162, which lies close to the substrate binding sites (i.e. 158 and 167) as well as within the region [97–237] required for repression of c-myc promoter activity [45]. Therefore, AGE modification of Lys-162 might impair both the enzymatic activity and non-glycolytic regulatory functions of ENO-1 in ccRCC cells. Clinically, low ENO1 expression in clear cell renal cell carcinoma has been associated with significantly decreased disease-free and overall survival [46], further highlighting the potential functional impact of ENO1 modification in cancer.

The second important enzyme, PKM2, exists in multiple oligomeric states: an inactive monomer, a low-activity dimer, and a highly active tetramer, which catalyzes the last step of glycolysis, transferring the phosphate from phosphoenolpyruvate (PEP) to ADP, yielding pyruvate and ATP [47]. Post-translational modifications of PKM2 such as phosphorylation, acetylation, or glycosylation

Table 3 A list of 21 proteins AGE-modified proteins at sites of or in close proximity of the functional domains unique to clear cell renal carcinoma (ccRCC) tissue of 16 patients grouped according to their main functions in biological processes

UniProt ID	Protein name (Symbol)	AGE adduct	Predicted modified site	Protein domains*	
				Position (s)	Function (s)
Glycolytic enzymes					
Q01813	ATP-dependent 6 phospho-fructokinase, platelet type (PFKP)	CEC or CMC	C-343	[1–399]	N-terminal catalytic PKF domain 1
P60174	Triosephosphate isomerase (TPI1)	Pento-s	K-238	[238]	PTM-lysine acetylation site
P04406	Glyceraldehyde 3-phosphate dehydrogenase (GAPDH)	CEL	K-186	[182] [186]	Substrate binding site (glyceraldehyde 3- phosphate) Glycyl lysine isopeptide (Gly-Lys) (interchain with G-Cter in SUMO 2)
P06733	Alpha enolase (ENO1)	CML or Pento-s	K-162	[158] [167] [97–237]	Substrate binding sites Region required for repression of myc promoter activity
P14618-1	Pyruvate kinase, isoform M2 (PKM2)	CEC	C-49	[44–166]	A1 domain; the interference between the A1 and B1 domains forms the catalytic active site
Oxidation–reduction processes					
V9HWC9	Superoxide dismutase [Cu–Zn] (HEL-S-44)	CMC	C-58	[15–150]	Sod-Cu domain
Transcription regulation and RNA processing					
Q53F64	Heterogeneous nuclear ribonucleoprotein AB isoform a variant	Pyr	K-92	[70–155]	RNA recognition motif (RRM)
Q08170	Serine/arginine-rich splicing factor 4 (SRSF4)	CMC	C-61	[2–72]	RRM1 domain
O60902	Short stature homeobox protein 2 (SHOX2)	Pyr	K-128, K-137	[140–199]	Homeobox DNA binding domain
R9QDZ0	Signal transducer and activator of transcription (STAT2)	CEC	C-594	[572–667]	SH2 domain interacts with phosphotyrosine-containing target peptides
Q9GZR2	RNA exonuclease 4 (REXO4)	Arg-p	R-392	[243–394]	Exonuclease domain
Protein folding					
P08238	Heat shock protein HSP 90-beta (HSP90AB1)	CMC	C-366	[366] [264–608]	Interacts with co-chaperone CDC37 Co-chaperone and client protein binding domain
A8K401	Prohibitin (PHB)	Pento-s	K-63, R-70	[26–187] [63]	Domain binds to newly synthesized mitochondrial proteins PTM—ubiquitination site
P30101	Protein disulfideisomerase A3 (PDIA3)	Pento-s	K-252	[252]	PTM—acetylation
Protein ubiquitination and degradation					
Q9GZZ9	Ubiquitin-like modifier-activating enzyme 5 (UBA5)	CEC	C-181	[183]	ATP binding site
Q16401	26S Proteasome non-ATP-ase regulatory subunit 5 (PSMD5)	CMC	C-361	[366–370]	Dileucin repeat (contributes to internalization and/or targeting 26S proteasome to membranes; contains ARM repeats that bind to PSMD2
Signaling pathway					
Q8IYD2	Kelch domain-containing protein 8A (KLHDC8A)	Arg-p	R-165	[128–175]	Kelch 4 repeat (protein–protein interactions)
P13385	Protein Cripto (CRIPTO)	CEC	C-115	[115 ↔ 133]	Disulfide bond
Immune responses					
P05156	Complement factor 1 (CFI)	Pento-s	K-19	[1–18]	Signal peptide
P22792	Carboxypeptidase N subunit 2 (CPN2)	Pento-s	R-98	[98–119]	Leucine-rich repeat (LRR1 repeat)
Blood coagulation					
P02749	Beta-2 glycoprotein 1 (APOH)	CEC	C-205	[205 ↔ 248]	Disulfide bond

*Protein domains were extracted from the UniProt database PTM, posttranslational modification

Used protein symbols come from the UniProtKB (2023), the full list of proteins (41) that formed AGE adducts at sites of or in close proximity of the functional domains in clear cell renal carcinoma (ccRCC) and corresponding non-tumor renal tissues is Additional File 8. Abbreviations: Arg-p, argpyrimidine; CEL-carboxyethyl-lysine; CML, carboxymethyl-lysine, CEC, carboxyethyl-cysteine; CMC, carboxymethyl-cysteine; Pento-s, pentosidine; Pyr, pyrraline

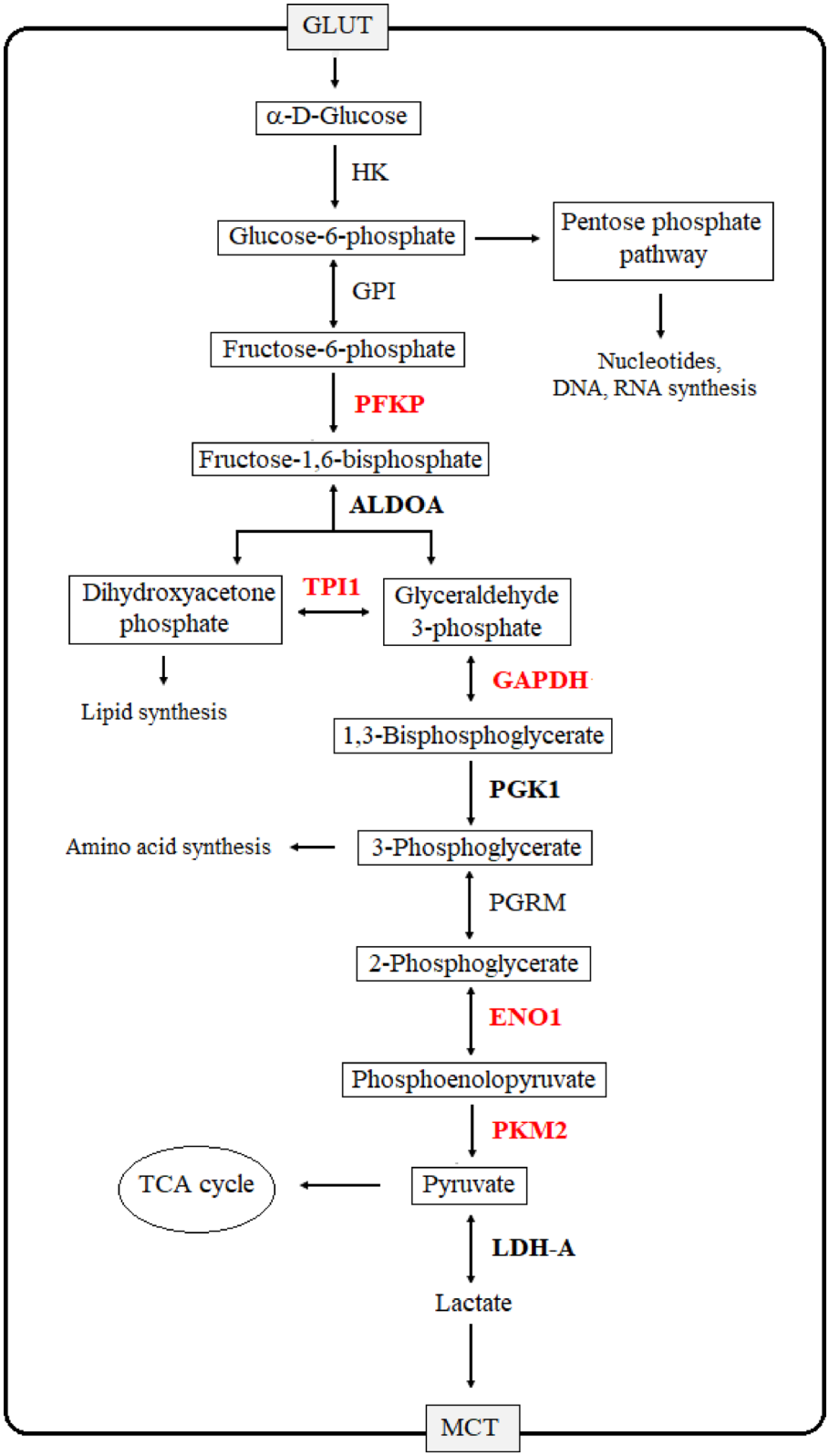

Fig. 7 Scheme of the role of AGE-modified proteins in glycolytic pathways. Enzymes found as modified by AGEs only in ccRCC tissue are highlighted **in red** and those in both tumor and non-tumor renal samples are **bold black**

have been shown to suppress PKM2 activity by disrupting tetramer formation, thereby promoting the Warburg effect and supporting anabolic growth in cancer cells [48]. In addition, dimeric PKM2 translocates to the nucleus, where it regulates gene expression by interacting with transcription factors. Previous studies have domonstrated that oxidation of Cys-358 or Cys-326 inhibits PKM2 by preventing the "intersubunit" interactions and reducing the formation of active tetramers in human lung cancer cells [49]. In our study, the AGE-PKM2 adduct was found at Cys-49 located in the A domain (residues 44–116 and 219–389), which is responsible for the subunit interaction and dimer formation [50]. Although the functional impact of Cys-49 glycation is not yet fully understood, its location within a structurally important domain suggests that such modification may alter PKM2 oligomerization and activity. Further studies are needed to determine whether AGE modification at this site contributes to PKM2 inactivation and whether it plays a role in the metabolic reprogramming of ccRCC cells.

It is also noteworthy that another multifunctional glycolytic enzyme, GAPDH was modified by CEL at Lys-186 located in close proximity to the substrate-binding site (i.e. 182) (Table 3). Of note, Lys-186 participates in the formation of an isopeptide bond with glycine at the C-terminus of SUMO-2 (small ubiquitin-like modifier-2) [51]. Sumoylation of GAPDH is known to regulate diverse cellular processes including cell signaling, cell cycle progression, and nuclear translocation [51]. Therefore, modification of Lys-186 by CEL may have dual consequences: interference with GAP binding and disruption of sumoylation, in cancer cells.

Mitochondrial proteins and redox processes

Other metabolic proteins that formed AGE adducts at sites or close to the functional domains include mitochondrial enzymes involved in ATP synthesis (i.e. ATP synthase protein 8; ATP8), the TCA cycle (succinate-CoA ligase subunit beta; SUCLG2), and lipid metabolism (i.e. membrane-associated phosphatidylinositol transfer protein 2; PITPNM2). Modifications of ATP8 and PITPNM2 by AGEs occurred in both ccRCC and non-tumor renal tissues, while SUCLG2 was modified only in non-tumor tissue. Because disturbances in mitochondrial processes are also associated with increased production of ROS, it was suggested that decreased activity of antioxidant enzymes may additionally contribute to the development and growth of kidney cancer [52]. The results obtained in our study indicate that four enzymes involved in oxidation–reduction processes, namely superoxide dismutase (Cu–Zn–SOD), glutathione peroxidase 4 (GPX 4), hydroxypyruvate reductase (GRHPR), and CYP2C9, were modified by AGEs exclusively in ccRCC (Table 2). Among these, the Cu,Zn-SOD, was modified by CMC at Cys-58, which lies within the SOD-Cu domain. Previous studies have shown that modification of Cu, Zn–SOD by GO or MGO leads to its inactivation [53]. Moreover, the antioxidant enzymes Cu, Zn–SOD, as well as glutathione peroxidase (GSH-Px) were previously shown to be downregulated in ccRCC tissues when compared to non-tumor tissue [54]. Another crucial antioxidant enzyme, catalase (CAT), was found to be modified by CEC on Cys-232, which lies close to the NADPH binding site [residue 237]. Because such modification certainly affects the activity of CAT [55], further studies are needed to determine the likely significance of this particular CAT modification in relation to the overall reduced antioxidant enzymatic activities caused by AGEs in ccRCC development.

Transcription regulation and RNA processing

Strong nuclear AGE staining in ccRCC samples suggests that AGEs can bind directly to DNA and/or DNA-associated proteins, causing their structural modifications. This might impair DNA repair mechanisms leading to mutations that promote tumorigenesis [18, 20, 21]. AGEs can also modify transcription factors in the nucleus, activate oncogenes or silence tumor suppressor genes. Both of which are strongly linked to tumor development. Many proteins that formed AGE adducts exclusively in ccRCC are known to be involved in transcription regulation and RNA processing in the nucleus (Table 3). These proteins include the previously discussed glycolytic enzymes (GAPDH, ENO1, and PKM2), as well as heterogeneous nuclear ribonucleoprotein AB (hnRNP AB) and serine/arginine-rich splicing factor 4 (SRSF4), which were modified within their RNA recognition motifs (RRMs) (Table 3). In addition, short stature homeobox protein 2 (SHOX2) was modified within its homeobox DNA-binding domain (Table 3). Although the functional consequences of these modifications remain to be elucidated, glycation within critical RNA- or DNA-binding domains could potentially impair transcriptional regulation, mRNA processing, or splicing processes essential for maintaining cellular homeostasis. The preferential occurrence of these modifications in tumor tissues suggests that glycation of nuclear proteins may contribute to the altered gene expression landscapes observed in renal cell carcinoma.

Heat shock proteins

An interesting finding of our proteomic analysis was the identification of AGE adducts on six proteins involved in protein folding, including the heat shock protein Hsp90β, prohibitin, and protein disulfide isomerase, which were modified by AGEs exclusively in the ccRCC tissues. The Hsp90β is an essential molecular chaperone involved in maintaining the stabilization and activity of many proteins, known as clients, in an ATP-dependent manner

[56]. Our results show that Hsp90β was modified by CEC at Cys-366, which is located within the co-chaperone and client protein-binding middle domain [residues 264–646]. Cys-366 is a highly reactive residue, which directly interacts with co-chaperone Cdc37p50. As a result, kinase-dependent protein degradation is observed, leading to cancer cell cycle arrest [57]. On the other hand, it was also demonstrated that MGO modification of Hsp90 in breast cancer cells reduces its binding to the client protein, i.e. the large tumor suppressor kinase 1 (LATS1), a key kinase of the Hippo pathway [58]. Consequently, a decreased expression of LATS1 and overexpression of the YAP oncogene have been demonstrated in many cancer types, including ccRCC [59].

On the other hand, mitochondrial heat shock protein 60 (HSPD1) appeared as modified at lysine-389 (CEL) both in non-tumor renal tissues and in ccRCC, which is known for low level of Hsp60 expression [60]. However, cancer might be promoted by AGEs affecting heat shock cognate 72 (HEL-S-72p), a protein that functions as a molecular chaperone, playing a crucial role in maintaining cellular protein homeostasis [61], while heat shock cognate 70 (Hsc70) was found to be modified by glyceraldehyde-derived AGEs and exhibits reduced activity in hepatocellular carcinoma cell lines [62]. Moreover, prohibitin was modified by pentosidine Arg-70 and Lys-63 located within the domain that binds to newly synthesized mitochondrial proteins, while Lys-63 is also known to be a ubiquitination site [63]. Therefore, such irreversible cellular protein modifications may interfere with important processes involving HSPs.

Protein ubiquitination and degradation

The 26S proteasome non-ATPase regulatory subunit 5 (PSMD5), found in our study modified by CEC on Cys-361 exclusively in ccRCC, forms a tetramer with Rpt1, Rpt2, and Rpn1 of the 19S proteasome regulator [35]. The Cys-361 is located close to the dileucine repeat [366–370], which contributes to internalization and/or targeting the 26S proteasome to membranes, while PSMD5 is a specific target in skin glycation during aging [36]. A previous study has demonstrated that PSMD5 acts as an inhibitor of 26S proteasome assembly, and its down-regulation/inactivation promotes 26S proteasome assembly during colorectal tumor progression [35]. Therefore, modifications of this protein could be studied as potential markers of carcinogenesis and a point of study for improving anti-cancer therapies.

The results of our study regarding the increase in AGEs levels in ccRCC tissue, as well as the results of recent studies from other groups, have shown that the formation of AGEs induced by low doses of MGO favors tumor growth in vivo [64], suggest potential benefits of partial reduction of AGEs by natural antioxidants, such as, e.g. carnosine [64]. This endogenous peptide reacts with MGO and glycated proteins, preventing the addition of protein carbonyls in cells under metabolic stress. Moreover, in vitro studies suggest that carnosine may be a potential anti-proliferative agent in renal carcinoma [65]. Similarly, the well-known antihyperglycemic drug metformin also reduces the formation of AGEs by reacting with α-dicarbonyl compounds [66], while it also reduces oxidative stress, inhibits the growth and migration of ccRCC cells, and improves survival of patients with localized RCC, although not in the case of metastatic RCC [67, 68].

Limitations

This study, presenting new data on protein modifications in the process of kidney carcinogenesis and their potential consequences, is burdened with some limitations. The presented results of immunofluorescent tissue staining and proteomic analysis only indicated which proteins and in what amounts are subject to modification, yet without assessing changes in their functionality resulting from impaired activity or regulation of biological pathways in which they participate. This limits the unambiguous interpretation and assessment of how the formation of AGE-protein adducts may contribute to the pathogenesis of ccRCC. Another significant limitation is the small number of patients from whom the material for the study was obtained, which prevents the creation of biostatistical models to transfer the obtained data to the entire population of patients with ccRCC. Despite the high incidence of this cancer, the availability of tissues collected during surgery that would meet the experimental requirements, including non-neoplastic tissue, is limited because during surgery the most important element is the patient's health, and collecting material for testing is only an addition. In addition, the removed cancerous tissue is primarily intended for histopathological examination, and only the remaining fragments, often relatively small to conduct analyses, can be used for scientific research. These are the reasons why we denote our findings as preliminary.

Conclusion

The results of this study revealed possibly important roles of the AGE-protein modifications in kidney carcinogenesis, notably the development of ccRCC. However, further investigation into the mechanisms underlying AGE-protein adduct formation in renal carcinogenesis is needed to increase our understanding of ccRCC metabolism and potentially contribute to improved diagnostic and therapeutic strategies.

Abbreviations

3-DG	3-Deoxyglucosone
ADP	Adenosine diphosphate

AGEs	Advanced glycation end products
AKT	Protein kinase B
ALDOA	Aldolase A
ATP	Adenosine triphosphate
ATP8	ATP synthase protein 8
CAT	Catalase
ccRCC	Clear cell renal cell carcinoma
CEC	S-(carboxyethyl) cysteine
CEL	Nε-(carboxyethyl) lysine
CKD	Chronic kidney disease
CMC	S-(carboxymethyl) cysteine
CML	Nε-(carboxymethyl) lysine
CPTAC	Clinical proteomic tumor analysis consortium
EDTA	Ethylenediaminetetraacetic acid
EGTA	Egtazic acid
ENO-1	Enolase 1
ERK	Extracellular signal-regulated kinase
FDR	False discovery rate
G6PD	Glucose-6-phosphate dehydrogenase
GAPDH	Glyceraldehyde 3-phosphate dehydrogenase
GAPDH	Glyceraldehyde-3-phosphate dehydrogenase
GO	Glyoxal
HIF	Hypoxia-inducible transcription factor
Hsc	Heat shock cognate
HSP	Heat shock protein
LATS1	Large tumor suppressor kinase 1
LDHA	Lactate dehydrogenase
MGO	Methylglyoxal
NF-κB	Nuclear factor kappa B
OXPHOS	Oxidative phosphorylation
PBS	Phosphate buffered saline
PEP	Phosphoenolpyruvate
PF	Phospho-fructokinase
PITPNM2	Membrane associated phosphatidylinositol transfer protein 2
PKM2	Pyruvate kinase M2
PPP	Pentose phosphate
PSMD5	26S proteasome non-ATPase regulatory subunit 5
PTMs	Post-translational modifications
RAGE	Receptor for advanced glycation end products
RRM	RNA recognition motif
SDS–PAGE	Sodium dodecyl-sulfate polyacrylamide gel electrophoresis
SHOX2	Short stature homeobox protein 2
SOD	Superoxide dismutase
SUCLG2	Succinate-CoA ligase subunit beta
TCA	Tricarboxylic acid
TNM	Tumor-node-metastasis
TPI	Triosephosphate isomerase
Tris/HCl	Tris(hydroxymethyl) aminomethane hydrochloride
VEGF	Vascular endothelial growth factor
VHL	*von Hippel-Lindau* Tumor suppressor gene

Supplementary Information

The online version contains supplementary material available at https://doi.org/10.1186/s12967-025-06958-6.

Additional file1

Additional file2

Additional file3

Additional file4

Additional file5

Additional file6

Additional file7

Additional file8

Author contributions

Conceptualization: HO, ES, NZ; Data curation: AG, JBJ, PS, RK; Formal Analysis: AG, JBJ, MK; Funding acquisition: ES; Investigation: AG, JBJ, RK; Methodology: AG, JBJ, PS; Project administration: ES; Software: AG, JBJ; Supervision: HO, NZ, ES; Validation: AG, JBJ, MK; Visualization: AG, JBJ; Writing – original draft: AG, HO, ES; Writing – review & editing: HO, NZ, ES. All authors have seen and approved the final version of the article.

Funding

The biochemical analysis carried out on cells was supported by the Ministry of Science and Higher Education (Poland) as part of the scientific activity of the Medical University of Bialystok. The funding body did not participate in the design of the study, analysis, or interpretation of data or in writing the manuscript.

Data availability

The mass spectrometry proteomics data have been deposited to the ProteomeXchange Consortium via the PRIDE [69] partner repository with the dataset identifier PXD059009.

Declarations

Ethics approval and consent to participate

All samples were obtained with informed patient consent and approval of the Human Care Committee of the Medical University of Bialystok (Poland) (No. R-I-002/43/2015).

Consent for publication

Not applicable.

Competing interests

The authors declare no conflict of interest. The funders had no role in the design of the study; in the collection, analyses, or interpretation of data; in the writing of the manuscript, or in the decision to publish the results.

Received: 14 April 2025 / Accepted: 30 July 2025
Published online: 14 August 2025

References

1. Padala SA, Barsouk A, Thandra KC, Saginala K, Mohammed A, Vakiti A, et al. Epidemiology of renal cell carcinoma. World J Oncol. 2020;11:79.
2. Peired AJ, Lazzeri E, Guzzi F, Anders H-J, Romagnani P. From kidney injury to kidney cancer. Kidney Int. 2021;100:55–66.
3. Shen C, Kaelin WG. The VHL/HIF axis in clear cell renal carcinoma. Semin Cancer Biol. 2013;23:18–25.
4. Bacigalupa ZA, Rathmell WK. Beyond glycolysis: Hypoxia signaling as a master regulator of alternative metabolic pathways and the implications in clear cell renal cell carcinoma. Cancer Lett. 2020;489:19–28.
5. Clark DJ, Dhanasekaran SM, Petralia F, Pan J, Song X, Hu Y, et al. Integrated proteogenomic characterization of clear cell renal cell carcinoma. Cell. 2019;179:964-983.e31.
6. Heiden MGV, Cantley LC, Thompson CB. Understanding the Warburg effect: the metabolic requirements of cell proliferation. Science. 2009;324:1029.
7. Pang L, Hou Y, Wang X, Du J, Huang H, Yang M, et al. Metabolic reprogramming of cancer stem cells and a novel eight-gene metabolism-related risk signature in clear cell renal carcinoma. Curr Chin Sci. 2024;4:72–84.
8. Wettersten HI, Aboud OA, Lara PN, Weiss RH. Metabolic reprogramming in clear cell renal cell carcinoma. Nat Rev Nephrol. 2017;13:410–9.
9. Paul S, Ghosh S, Kumar S. Tumor glycolysis, an essential sweet tooth of tumor cells. Semin Cancer Biol. 2022;86:1216–30.
10. Sawant Dessai A, Kalhotra P, Novickis AT, Dasgupta S. Regulation of tumor metabolism by post translational modifications on metabolic enzymes. Cancer Gene Ther. 2023;30:548–58.
11. Martin MS, Jacob-Dolan JW, Pham VTT, Sjoblom NM, Scheck RA. The chemical language of protein glycation. Nat Chem Biol. 2025;21:324–36.
12. Lin J-A, Wu C-H, Lu C-C, Hsia S-M, Yen G-C. Glycative stress from advanced glycation end products (AGEs) and dicarbonyls: an emerging biological factor in cancer onset and progression. Mol Nutr Food Res. 2016;60:1850–64.

13. Wang F, Zhao Y, Niu Y, Wang C, Wang M, Li Y, et al. Activated glucose-6-phosphate dehydrogenase is associated with insulin resistance by upregulating pentose and pentosidine in diet-induced obesity of rats. Horm Metab Res. 2012;44:938–42.
14. Rondeau P, Bourdon E. The glycation of albumin: Structural and functional impacts. Biochimie. 2011;4:645–58.
15. Zhang Q, Tang N, Schepmoes AA, Phillips LS, Smith RD, Metz TO. Proteomic profiling of nonenzymatically glycated proteins in human plasma and erythrocyte membranes. J Proteome Res. 2008;7:2025–32.
16. Oya-Ito T, Naito Y, Takagi T, Handa O, Matsui H, Yamada M, et al. Heat-shock protein 27 (Hsp27) as a target of methylglyoxal in gastrointestinal cancer. Biochim Biophys Acta. 2011;1812:769–81.
17. Irshad Z, Xue M, Ashour A, Larkin JR, Thornalley PJ, Rabbani N. Activation of the unfolded protein response in high glucose treated endothelial cells is mediated by methylglyoxal. Sci Rep. 2019;9:7889.
18. Sanghvi VR, Leibold J, Mina M, Mohan P, Berishaj M, Li Z, et al. The oncogenic action of NRF2 depends on de-glycation by fructosamine-3-kinase. Cell. 2019;178:807-819.e21.
19. Morgan PE, Dean RT, Davies MJ. Inactivation of cellular enzymes by carbonyls and protein-bound glycation/glycoxidation products. Arch Biochem Biophys. 2002;403:259–69.
20. Sun F, Suttapitugsakul S, Xiao H, Wu R. Comprehensive analysis of protein glycation reveals its potential impacts on protein degradation and gene expression in human cells. J Am Soc Mass Spectrom. 2019;30:2480–90.
21. Donnellan L, Young C, Simpson BS, Acland M, Dhillon VS, Costabile M, et al. Proteomic analysis of methylglyoxal modifications reveals susceptibility of glycolytic enzymes to dicarbonyl stress. Int J Mol Sci. 2022;23:3689.
22. Rungratanawanich W, Qu Y, Wang X, Essa MM, Song B-J. Advanced glycation end products (AGEs) and other adducts in aging-related diseases and alcohol-mediated tissue injury. Exp Mol Med. 2021;53:168–88.
23. Bellier J, Nokin M-J, Lardé E, Karoyan P, Peulen O, Castronovo V, et al. Methylglyoxal, a potent inducer of AGEs, connects between diabetes and cancer. Diabetes Res Clin Pract. 2019;148:200–11.
24. Chiavarina B, Nokin M-J, Durieux F, Bianchi E, Turtoi A, Peulen O, et al. Triple negative tumors accumulate significantly less methylglyoxal specific adducts than other human breast cancer subtypes. Oncotarget. 2014;5:5472–82.
25. Jabir NR, Ahmad S, Tabrez S. An insight on the association of glycation with hepatocellular carcinoma. Semin Cancer Biol. 2018;49:56–63.
26. Senavirathna L, Pan S, Chen R. Protein advanced glycation end products and their implications in pancreatic cancer. Cancer Prev Res Phila. 2023;16:601–10.
27. Fischer A, Correa-Gallegos D, Wannemacher J, Christ S, Machens H-G, Rinkevich Y. In vivo fluorescent labeling and tracking of extracellular matrix. Nat Protoc. 2023;18:2876–90.
28. Greifenhagen U, Nguyen VD, Moschner J, Giannis A, Frolov A, Hoffmann R. Sensitive and site-specific identification of carboxymethylated and carboxyethylated peptides in tryptic digests of proteins and human plasma. J Proteome Res. 2015;14:768–77.
29. Chong J, Wishart DS, Xia J. Using MetaboAnalyst 4.0 for comprehensive and integrative metabolomics data analysis. Curr Protoc Bioinformatics. 2019;68:e86.
30. Thomas PD, Ebert D, Muruganujan A, Mushayahama T, Albou L-P, Mi H. PANTHER: making genome-scale phylogenetics accessible to all. Protein Sci. 2022;31:8–22.
31. CPTAC-CCRCC [Internet]. The Cancer Imaging Archive (TCIA). [cited 2025 Jul 3]. Available from: https://www.cancerimagingarchive.net/collection/cptac-ccrcc/
32. Rabbani N, Thornalley PJ. Advanced glycation end products in the pathogenesis of chronic kidney disease. Kidney Int. 2018;93:803–13.
33. Dey S, Hamilton Z, Noyes SL, Tobert CM, Keeley J, Derweesh IH, et al. Chronic kidney disease is more common in locally advanced renal cell carcinoma. Urology. 2017;105:101–7.
34. Wagner MC, Myslinski J, Pratap S, Flores B, Rhodes G, Campos-Bilderback SB, et al. Mechanism of increased clearance of glycated albumin by proximal tubule cells. Am J Physiol Renal Physiol. 2016;310:F1089-1102.
35. Merlot AM, Kalinowski DS, Richardson DR. Unraveling the mysteries of serum albumin-more than just a serum protein. Front Physiol. 2014;5: 299.
36. Ahmed A, Shamsi A, Khan MS, Husain FM, Bano B. Methylglyoxal induced glycation and aggregation of human serum albumin: biochemical and biophysical approach. Int J Biol Macromol. 2018;113:269–76.
37. Guo Y, Zhang H-C, Xue S, Zheng J-H. Receptors for advanced glycation end products is associated with autophagy in the clear cell renal cell carcinoma. J Cancer Res Ther. 2019;15:317–23.
38. Wa C, Cerny RL, Clarke WA, Hage DS. Characterization of glycation adducts on human serum albumin by matrix-assisted laser desorption/ionization time-of-flight mass spectrometry. Clin Chim Acta. 2007;385:48–60.
39. Ware LB, Johnson ACM, Zager RA. Renal cortical albumin gene induction and urinary albumin excretion in response to acute kidney injury. Am J Physiol Renal Physiol. 2011;300:F628-638.
40. Nahon JL, Tratner I, Poliard A, Presse F, Poiret M, Gal A, et al. Albumin and alpha-fetoprotein gene expression in various nonhepatic rat tissues. J Biol Chem. 1988;263:11436–42.
41. Peters T, Davidson LK. The biosynthesis of rat serum albumin. In vivo studies on the formation of the disulfide bonds. J Biol Chem. 1982;257:8847–53.
42. Kragh-Hansen U, Minchiotti L, Galliano M, Peters T. Human serum albumin isoforms: genetic and molecular aspects and functional consequences. Biochim Biophys Acta. 2013;1830:5405–17.
43. Chougale AD, Bhat SP, Bhujbal SV, Zambare MR, Puntambekar S, Somani RS, et al. Proteomic analysis of glycated proteins from streptozotocin-induced diabetic rat kidney. Mol Biotechnol. 2012;50:28–38.
44. Bansode SB, Chougale AD, Joshi RS, Giri AP, Bodhankar SL, Harsulkar AM, et al. Proteomic analysis of protease resistant proteins in the diabetic rat kidney. Mol Cell Proteomics. 2013;12:228–36.
45. Didiasova M, Schaefer L, Wygrecka M. When place matters: shuttling of enolase-1 across cellular compartments. Front Cell Dev Biol. 2019;7:61.
46. White-Al Habeeb NM, Di Meo A, Scorilas A, Rotondo F, Masui O, Seivwright A, et al. Alpha-enolase is a potential prognostic marker in clear cell renal cell carcinoma. Clin Exp Metastasis. 2015;32:531–41.
47. Yang W, Lu Z. Pyruvate kinase M2 at a glance. J Cell Sci. 2015;128:1655–60.
48. Hitosugi T, Chen J. Post-translational modifications and the Warburg effect. Oncogene. 2014;33:4279–85.
49. Anastasiou D, Poulogiannis G, Asara JM, Boxer MB, Jiang J, Shen M, et al. Inhibition of pyruvate kinase M2 by reactive oxygen species contributes to cellular antioxidant responses. Science. 2011;334:1278–83.
50. Prakasam G, Iqbal MA, Bamezai RNK, Mazurek S. Posttranslational modifications of pyruvate kinase M2: tweaks that benefit cancer. Front Oncol. 2018;8:22.
51. Hendriks IA, Lyon D, Young C, Jensen LJ, Vertegaal ACO, Nielsen ML. Site-specific mapping of the human SUMO proteome reveals co-modification with phosphorylation. Nat Struct Mol Biol. 2017;24:325–36.
52. Pljesa-Ercegovac M, Mimic-Oka J, Dragicevic D, Savic-Radojevic A, Opacic M, Pljesa S, et al. Altered antioxidant capacity in human renal cell carcinoma: role of glutathione associated enzymes. Urol Oncol. 2008;26:175–81.
53. Kang JH. Modification and inactivation of human Cu,Zn-superoxide dismutase by methylglyoxal. Mol Cells. 2003;15:194–9.
54. Zacchia M, Vilasi A, Capasso A, Morelli F, De Vita F, Capasso G. Genomic and proteomic approaches to renal cell carcinoma. J Nephrol. 2011;24:155–64.
55. Nagarkoti S, Dubey M, Awasthi D, Kumar V, Chandra T, Kumar S, et al. S-glutathionylation of p47phox sustains superoxide generation in activated neutrophils. Biochimica et Biophysica Acta (BBA). 2018;1865:444–54.
56. Taherian A, Krone PH, Ovsenek N. A comparison of Hsp90α and Hsp90β interactions with cochaperones and substrates. Biochem Cell Biol. 2008;86:37–45.
57. Zhang FZ, Ho DH-H, Wong RH-F. Triptolide, a HSP90 middle domain inhibitor, induces apoptosis in triple manner. Oncotarget. 2018;9:22301.
58. Nokin M-J, Durieux F, Peixoto P, Chiavarina B, Peulen O, Blomme A, et al. Methylglyoxal, a glycolysis side-product, induces Hsp90 glycation and YAP-mediated tumor growth and metastasis. Elife. 2016;5: e19375.
59. Rybarczyk A, Klacz J, Wronska A, Matuszewski M, Kmiec Z, Wierzbicki PM. Overexpression of the *YAP1* oncogene in clear cell renal cell carcinoma is associated with poor outcome. Oncol Rep. 2017;38:427–39.
60. Tang H, Chen Y, Liu X, Wang S, Lv Y, Wu D, et al. Downregulation of HSP60 disrupts mitochondrial proteostasis to promote tumorigenesis and progression in clear cell renal cell carcinoma. Oncotarget. 2016;7:38822.
61. Cai J, Tao Z, Chen X, Yi S. Identification and analysis of transcriptional regulatory networks of osteosarcoma microarray data via systems biology. J Oleo Sci. 2022;71:379.
62. Takino J-I, Yamagishi S-I, Takeuchi M. Cancer malignancy is enhanced by glyceraldehyde-derived advanced glycation end-products. J Oncol. 2010;2010: 739852.
63. Sun F, Kanthasamy A, Anantharam V, Kanthasamy AG. Mitochondrial accumulation of polyubiquitinated proteins and differential regulation of apoptosis by polyubiquitination sites Lys-48 and -63. J Cell Mol Med. 2009;13:1632–43.
64. Nokin M-J, Durieux F, Bellier J, Peulen O, Uchida K, Spiegel DA, et al. Hormetic potential of methylglyoxal, a side-product of glycolysis, in switching tumours from growth to death. Sci Rep. 2017;7:11722.

65. Pandurangan M, Enkhtaivan G, Kim DH. Therapeutic efficacy of natural dipeptide carnosine against human cervical carcinoma cells. J Mol Recognit. 2016;29:426–35.
66. Ruggiero-Lopez D, Lecomte M, Moinet G, Patereau G, Lagarde M, Wiernsperger N. Reaction of metformin with dicarbonyl compounds. Possible implication in the inhibition of advanced glycation end product formation. Biochem Pharmacol. 1999;58:1765–73.
67. Cheng JJS, Li H, Tan HS, Tan PH, Ng LG, Ng QS, et al. Metformin use in relation with survival outcomes of patients with renal cell carcinoma. Clin Genitourin Cancer. 2016;14:168–75.
68. Zhang Y, Zhang S, Sun H, Xu L. The pathogenesis and therapeutic implications of metabolic reprogramming in renal cell carcinoma. Cell Death Discov. 2025;11:186.
69. Perez-Riverol Y, Bai J, Bandla C, García-Seisdedos D, Hewapathirana S, Kamatchinathan S, et al. The PRIDE database resources in 2022: a hub for mass spectrometry-based proteomics evidences. Nucleic Acids Res. 2021;50:D543–52.

Publisher's note